Measurement of Wigner function via atomic beam deflection in Raman-Nath regime

Ashfaq Hussain Khosa[(1)] and M. Suhail Zubairy[(1,2)]

(1) *Department of Electronics, Quaid-i-Azam University, Islamabad, Pakistan.*

(2) *Department of Physics, Texas A & M University, College Station Texas, 77843, USA.*

Abstract

We propose a method for the reconstruction of photon statistics and hence the Wigner function of a quantized cavity field. The method is based on the measurement of momentum distribution of two level atoms after atom-field interaction in Raman-Nath regime. We reconstruct the photon statistics of the cavity field both the cases of resonant and off-resonant atom field interaction.. For the measurement of Wigner function we propose to displace the photon statistics of the cavity field. We successfully reconstruct the Wigner function of the Schrödinger-cat state in a straightforward manner by employing the proposed method without much mathematical manipulation of the experimental data.

I. INTRODUCTION

The concept of a quantum state has always played a key role in discussions treating the foundations of quantum theory. Each physical quantity can be represented by a Hermitian operator which is called an 'observable' [1,2]. A measurement of this observable leaves the system in an eigenstate of the operator. A single measurement performed on a quantum system reveals a certain aspect of its state, and it will not uncover the quantum state completely. However, if we know how to determine the whole set of potentialities, the quantum state can be recovered [3]. It is a basic assumption of the quantum theory that an infinite ensemble of system contains all the information about the quantum system.

The quantum state of the radiation field is described completely by the state vector $|\psi\rangle$ for a pure state and by the density operator ρ for a more general mixed state. Equivalent descriptions of the quantum state can be formulated in terms of the quasiprobability distributions such as P-representation, Q-representation or the Wigner distribution function. These distributions, which do not have all the properties of a classical probability distribution, allow the evaluation of various correlation functions of the field operators, using the methods of classical statistical mechanics. For example, the Wigner distribution function affords the evaluation of symmetrically ordered correlation functions of the creation and destruction operators of the field. In recent years, a large class of the states of the radiation field have been studied. Some of them such as a squeezed state [4] or a Schrödinger-cat state [5] exhibit interesting features in their quantum statistical properties, for example, they may have oscillatory photon distributions.

Several methods have been proposed to measure quantum state of light as well as quantum state of matter. One method that allows us to perform measurements on wave function is the so-called tomographic method [6,7]. In this method, the distribution for the electric field quadrature amplitudes are measured via optical homodyne measurements and the Wigner distribution function of the radiation field is constructed from these measurements via Radon transformation. This method has been realized experimentally. The other meth-

ods which allow us to determine the quantum state of an electromagnetic field in a cavity or quantum state of matter are based on the fundamental interaction of atoms with the cavity field. These include methods based on dispersive atom-field coupling in a Ramsey method of separated oscillatory fields [8], atomic beam deflection [9–11] and the conditional measurements on the atoms in a micromaser setup [12]. A class of schemes for the measurement of the quantum state of the radiation field involves the measurement of the absorption and emission spectrum in a driven system [13,14]. The atom deflection method [10,11] uses momentum distribution of atoms in order to reveal the quantum state of the light inside the cavity. In this case, the atom serves as a tool that probes a quantum state of radiation field.

Freyberger and Herkommer proposed an intresting scheme for the measurement of quantized cavity field [11]. Their proposed scheme utilizes resonant two-level atoms. The atoms are prepared in coherent superposition of atomic internal states before interacting with the cavity field which is to be measured. They put a narrow slit of width much smaller than the wavelength of the cavity field in front of standing wave (of the cavity field). Under this approximation, $\sin(k\hat{x})$ dependence can be replaced by linear $k\hat{x}$ dependence in the interaction Hamiltonian. They have studied the momentum distribution of the atoms and found the photon statistics of the cavity field by the recursion relation $w_m = a/w^*_{m-1}$. The scheme works well for the case where the probability amplitudes of photon statistics never go to zero. On the other hand it has limitations that w_m cannot be found when the probability amplitude w^*_{m-1} becomes equal to zero. Such is, for example, in the case of Schrödinger-cat state which has an oscillatory photon statistics.

Another scheme proposed by Schneider *et al.* [20] also takes into account the atomic deflection method for the reconstruction of the quantized cavity field. They make use of a strong coherent reference field travelling orthogonally with respect to the cavity mode. The strong coherent field plays a similar role as the local oscillator in the homodyne tomography [21,22]. While their passage through the cavity, the atomic probe interacts for a short time with the cavity and the reference field. They measure the momentum distribution

of the atoms for different phases of the classical field and reconstruct an s-parametrized quasiprobability distribution of the field.

The scheme we propose utilizes a beam of two-level atoms in their ground state. We observe that the momentum distribution of the atoms, after interacting with the cavity field can be used for the reconstruction of photon statistics and hence the Wigner function of the cavity field. Contrary to Freyberger and Herkommer [11], our proposal do not require the superposition of atomic states, rather than this we inject a coherent state inside the cavity which causes the displacement of the original photon statistics of the field. The cavity field is coupled to a resonant classical oscillator for the displacement of photon statistics of it. The role of this coupling in the quantum state measurement has been discussed in Ref. [15]. The Wigner function is reconstructed in a completely different way and the mathematical framework is more simpler.

In section II, we derive expression for the Wigner function of the cavity field in terms of displaced photon statistics. We also discuss the role of the derived expression used to reconstruct the photon statistics of the cavity field. In section III, resonant atom-field interaction is discussed. We recover the photon statistics of the Schrödinger-cat state and also reconstruct the Wigner function for the same. The section IV deals with the off-resonant atom-field interaction, where we again reconstruct the photon statistics and Wigner function of the cavity field. It is very interesting to note that in non-demolition interaction of the off-resonant case, the mathematics is much simpler. Section V presents conclusion of the proposed model.

II. WIGNER FUNCTION OF THE RADIATION FIELD

In order to measure the Wigner function of the cavity field we assume that there is a probability $p(m)$ of m photons inside the cavity. The schematics of the proposed scheme is shown in Fig. 1. A classical oscillator is connected to the cavity so that it injects a coherent state inside it. The injection of the coherent state causes the displacement of the field. The

displacement operator $D(\alpha)$, is defined as

$$D\left(\alpha\right)=\exp\left[\alpha a^{\dagger}\ -\alpha^{*}a\right]. \tag{1}$$

We recall the definition of the quasiprobability distribution, which belongs to a general class of phase-space distribution [16,17] and reads as

$$\Phi(\alpha,\alpha^{*})=\frac{1}{\pi}\mathrm{Tr}[\rho T(\alpha,s)], \tag{2}$$

where s is the order of products of field operators. By order we mean the normal order (all creation operators i.e., $a^{\dagger}$ on left of the annihilation operators a), antinormal order (all creation operators i.e., $a^{\dagger}$ on right of the annihilation operators a) and symmetric order. The $s=1,-1$, or 0 for normal-, antinormal-, and symmetric-order, respectively. The term $T(\alpha,s)$ which is given by [17]

$$T(\alpha,s)=\frac{1}{\pi}\int\exp\left[\beta^{*}\alpha-\beta\alpha^{*}\right]\exp\left[\frac{s\left|\beta\right|^{2}}{2}\right]D(\beta)\ d^{2}\beta, \tag{3}$$

is the Fourier transform of the displacement operator $D(\beta)$. For $s=0$ one obtains the Wigner distribution function and for $s=-1$, and 1, $Q-$representation and $P-$representation, respectively. An alternative expression for $T(\alpha,s)$, which is useful for the present purpose is given by [17]

$$T(\alpha,s)=\frac{2}{1-s}D(\alpha)\left(\frac{s+1}{s-1}\right)^{a^{\dagger}a}D^{\dagger}(\alpha).$$

For the Wigner function (as $s=0$), the $T(\alpha,0)$ is

$$T(\alpha,0)=2D(\alpha)\left(-1\right)^{a^{\dagger}a}D^{\dagger}(\alpha).$$

The quasiprobability distribution defined in equation (2) is called the Wigner distribution function in this case and it obtains the form

$$W(\alpha,\alpha^{*})=\frac{2}{\pi}\sum_{m}\left(-1\right)^{m}\mathrm{Tr}[\rho D(\alpha)\left|m\right\rangle\left\langle m\right|D^{\dagger}(\alpha)]. \tag{4}$$

For a general state $\rho=\left|\Psi\right\rangle\left\langle\Psi\right|$, we obtain the following expression

$$W(\alpha,\alpha^*)=\frac{2}{\pi}\sum_m(-1)^m p(m,\alpha), \tag{5}$$

where $p(m,\alpha)$ is the displaced photon statistics of the cavity field, i.e.,

$$p(m,\alpha)=|\langle m|D^\dagger(\alpha)|\Psi\rangle|^2. \tag{6}$$

Thus the Wigner function of the cavity field can be found directly if the displaced photon statistics $p(m,\alpha)$ is known for all values of α. In this paper, we first find out the photon statistics and then the Wigner characteristic function of the cavity field with the help of displaced photon statistics.

III. RESONANT ATOM-FIELD INTERACTION

In this section we consider the same scheme as that of Freyberger and Herkommer [11] with two modifications: (a) we inject two-level atoms in the standing wave cavity field in their ground state $|b\rangle$ and (b) we displace the photon statistics of the cavity field by injecting a coherent state for the measurement of the Wigner function. We take the transition $|a\rangle-|b\rangle$ of the two-level atom resonant with the single mode quantized cavity field. A narrow slit of width δx placed in front of the cavity allows the atoms to collimate on a small region of the cavity field. Further, we consider the interaction in Raman-Nath regime where the kinetic energy term in Hamiltonian can be neglected. The interaction picture Hamiltonian in dipole and rotating-wave approximations is given by

$$H\ =\hbar gk\hat{x}(\sigma_+a+a^\dagger\sigma_-), \tag{7}$$

where a and $a^\dagger$ represent the annihilation and creation operators of the driving cavity field of wave vector $k=2\pi/\lambda$, respectively. The term g stands for the vacuum Rabi frequency and $\sigma_+(\sigma_-)$ is the usual atomic raising (lowering) operator. The atoms are transmitted through the opening of the slit. We approximate that the opening is very small as compared to the wave length of the cavity field (i.e., $\delta x\ll\lambda$) and is centered around $x=0$. Due to

this approximation we have replaced the usual $\sin(k\hat{x})$ dependence of the standing wave of cavity field by a linear $k\hat{x}$ dependence.

The equations of motion for the density matrix elements for the present case are

$$\dot{\rho}_{a,a}^{m-1,m-1}(x',x,t) = igk\sqrt{m}\left\{x\rho_{a,b}^{m-1,m}(x',x,t) - x'\rho_{b,a}^{m,m-1}(x',x,t)\right\}, \tag{8}$$

$$\dot{\rho}_{a,b}^{m-1,m}(x',x,t) = igk\sqrt{m}\left\{x\rho_{a,a}^{m-1,m-1}(x',x,t) - x'\rho_{b,b}^{m,m}(x',x,t)\right\}, \tag{9}$$

$$\dot{\rho}_{b,a}^{m,m-1}(x',x,t) = igk\sqrt{m}\left\{x\rho_{b,b}^{m,m}(x',x,t) - x'\rho_{a,a}^{m-1,m-1}(x',x,t)\right\}, \tag{10}$$

$$\dot{\rho}_{b,b}^{m,m}(x',x,t) = igk\sqrt{m}\left\{x\rho_{b,a}^{m,m-1}(x',x,t) - x'\rho_{a,b}^{m-1,m}(x',x,t)\right\}, \tag{11}$$

where m represents the number of photons inside the cavity. The set of coupled differential equations for density matrix elements can be solved by using the method given in Ref. [16], which needs to write the equations in terms of matrix equation i.e.,

$$\dot{R}(t) = -MR(t), \tag{12}$$

where $R(t)$ is the column vector of density matrix elements and M is the matrix of the coefficients. To solve equation (12), we need the eigenvalues and eigenvectors of matrix M. The eigenvalues of matrix M are $E_1 = -N(x-x')$, $E_2 = N(x+x')$, $E_3 = -N(x+x')$, and $E_4 = N(x-x')$ with $N = igk\sqrt{m}$. The matrix $V = [\, V_1 \;\; V_2 \;\; V_3 \;\; V_4 \,]$ of the eigenvectors satisfies the identity $VV^{-1} = 1$. The solution of the equation (12) is given by

$$R(t) = (V^{-1}e^{-D\ t}V)R(0), \tag{13}$$

where D is diagonalized matrix having eigenvalues of M as its diagonal elements.

We consider $g(x)$ to be the initial position distribution function of atoms at the slit. The modulus square of $g(x)$ gives the probability of finding the atom at position x. We have supposed that the photon statistics of the cavity field is $p(m)$, and the atoms are injected in their ground state. This in turn makes the initial condition that the initial probabilities of all the density matrix elements other than the ground state are zero, i.e.,

$$\rho_{a,a}^{m-1,m-1}(x',x,0) = \rho_{a,b}^{m-1,m}(x',x,0) = \rho_{b,a}^{m,m-1}(x',x,0) = 0. \tag{14}$$

As the probability of the ground stated atoms equate to one and the system is unentangled at $t = 0$, we can write

$$\rho_{b,b}^{m,m}(x', x, 0) = g(x')g(x)p(m). \tag{15}$$

The equations of motion of the density matrix elements (i.e., 8-11) are solved subject to initial conditions (14) and (15). The resultant equations of the density matrix elements are

$$\rho_{a,a}^{m-1,m-1}(x', x, t) = -\frac{1}{2}\left\{\cos(Q) - \cos(P)\right\} g(x')g(x)p(m), \tag{16}$$

$$\rho_{a,b}^{m-1,m}(x', x, t) = \frac{i}{2}\left\{\sin(Q) - \sin(P)\right\} g(x')g(x)p(m), \tag{17}$$

$$\rho_{b,a}^{m,m-1}(x', x, t) = -\frac{i}{2}\left\{\sin(Q) + \sin(P)\right\} g(x')g(x)p(m), \tag{18}$$

$$\rho_{b,b}^{m,m}(x', x, t) = \frac{1}{2}\left\{\cos(Q) + \cos(P)\right\} g(x')g(x)p(m), \tag{19}$$

where $Q = g\sqrt{m}(x + x')t$ and $P = g\sqrt{m}(x - x')t$. In order to measure the momentum distribution of the atoms, for the proposed experiment, we take the Fourier transform from position space to momentum space in normalized co-ordinates as

$$\rho(\wp, t) = \frac{1}{2\pi\hbar}\int_{-\infty}^{\infty}\frac{d\theta}{k}\int_{-\infty}^{\infty}\frac{d\theta'}{k}\rho(\theta', \theta, t)\exp\left[i\wp\left(\theta' - \theta\right)\right]. \tag{20}$$

Where $\wp = p/\hbar k$ and $\theta = kx$ denote the normalized momentum and position, respectively. Note that the atomic states, the field states and the position states of the atoms are entangled at this stage. We are interested in the momentum distribution of the atoms and hence do not bother about the internal states of the atoms and the cavity field states. This is done by taking the trace over the field states and the internal states of the atoms, which leads to the probability of the momentum distribution on the detection screen and is given by

$$W(\wp) = \sum_{m}\left[\rho_{a,a}^{m,m}\left(\wp, t\right) + \rho_{b,b}^{m,m}\left(\wp, t\right)\right]. \tag{21}$$

On substituting the values of $\rho_{a,a}^{m,m}\left(\wp, t\right)$ and $\rho_{b,b}^{m,m}\left(\wp, t\right)$, equation (21) can be casted as

$$W(\wp) = 2\sum_{m}\left[\left(\left|f(\wp + \kappa\sqrt{m})\right|^2 + \left|f(\wp - \kappa\sqrt{m})\right|^2\right)p(m)\right], \tag{22}$$

where

$$f(\wp \pm \kappa\sqrt{m}) = \frac{1}{2\sqrt{2\pi\hbar}} \int_{-\infty}^{\infty} \frac{d\theta}{k} g\left(\frac{\theta}{k}\right) \exp\left[-i(\wp \pm \kappa\sqrt{m})\theta\right], \tag{23}$$

is the Fourier transform of the position distribution function with $\kappa = gt$, and $g\left(\frac{\theta}{k}\right)$ being the position distribution of the atoms at the slit.

As an example, while measuring photon statistics of the cavity field we take the normalized Gaussian distribution of the atoms at the slit

$$g\left(\frac{\theta}{k}\right) = \left(\frac{1}{\pi\delta x^2}\right)^{\frac{1}{4}} \exp\left[-\theta^2 k^{-2}/2\delta x^2\right]. \tag{24}$$

Using equation (24) in (23) and integrating, we get

$$f(\wp \pm \kappa\sqrt{m}) = \left(\frac{\delta x^2}{16\pi\hbar^2}\right)^{\frac{1}{4}} \exp\left[-k^2\delta x^2(\wp \pm \kappa\sqrt{m})^2/2\right]. \tag{25}$$

The plots of $W(\wp)$ versus $\wp/\kappa$ shows that the first term in equation (22) corresponds to the negative side of $\wp/\kappa$ axis and second term corresponds to the positive side. It is clear from equation (25) that the peaks will appear when $\wp/\kappa$ equates $\sqrt{m}$. For $\sqrt{m} = 0$, the contribution comes from both the terms of the equation, i.e., $|f(\wp + \kappa\sqrt{m})|^2$ and $|f(\wp - \kappa\sqrt{m})|^2$, hence the peak located at $\wp/\kappa = 0$ has the double height. For the situation where $\kappa k \delta x \gg 0$, the $f(\wp \pm \kappa\sqrt{m})$ is a sharply peaked function at $\wp/\kappa = \pm\sqrt{m}$. To show this behavior we let that the Schrödinger-cat state is present in the cavity. The photon statistics of it is given by

$$p(m) = \frac{|\xi|^{2m}\left(1 + (-1)^m\right) \exp\left[|\xi|^2\right]}{\mathcal{N}' m!}, \tag{26}$$

with $\mathcal{N}' = 1 + e^{-2|\xi|^2}$is the normalizing constant and ξ is the average number of photons in the cavity mode. Fig. $2(a)$ shows the plot of the original photon statistics of Schrödinger-cat state for $\xi = 3$. We find the momentum distribution for different values of κ and recover the photon statistics for these values. It is noted that when the value of κ is increased graduelly, the peaks in the momentum distribution spectrum begain to resolve. We recover the photon statistics of the cavity field from the different momentum distribution spectrums

cooresponding to values of κ. The graphs in Fig. 3 show that for sufficient large κ, the photon statistics of the cavity field can be fully recovered.

For the reconstruction of Wigner function of the cavity field, we inject a coherent state inside the cavity, which displaces the original photon statistics of the field in phase space. This displaced photon statistics of the cavity field $p_r(m,\alpha)$ is recovered from the momentum distribution $W(\wp)$ via

$$p_r(m,\alpha) = \begin{cases} \frac{1}{2\mathcal{N}} W(\wp)|_{\wp=0} & \text{for } m=0, \\ \frac{1}{\mathcal{N}} W(\wp)|_{\wp=\kappa\sqrt{m}} & \text{for } m \geq 1, \end{cases} \tag{27}$$

where $\mathcal{N}$ is a normalization constant to ensure $\Sigma_m p_r(m,\alpha) = 1$. The factor 2 in the denominator, for the case where $m = 0$, comes due to the contribution from both the terms (see equation (22)). The displaced photon statistics of the cavity field can be recovered using the same method as discussed above. We use equation (5) for the reconstruction of the Wigner function of cavity field after finding the displaced photon statistics.

As an example of the recovery of the Wigner function we take a Schrödinger-cat state present in the cavity, and is expressed as

$$|\Psi\rangle = \mathcal{N}^{'}(|\alpha_0\rangle + |-\alpha_0\rangle). \tag{28}$$

The photon distribution of the Schrödinger-cat state after the injection of coherent state $|\alpha\rangle$ into the cavity is obtained

$$p(m,\alpha) = |\mathcal{M}|^2[p^{(+)}(m,\alpha) + p^{(-)}(m,\alpha) + \varepsilon(m,\alpha)], \tag{29}$$

where

$$\begin{aligned} p^{(+)}(m,\alpha) &= |\langle m|D^{\dagger}(\alpha)|\alpha_0\rangle|^2 \\ &= (m!)^{-1}|\alpha_0-\alpha|^{2m}\exp\left[-|\alpha|^2-|\alpha_0|^2+\alpha\alpha_0^*+\alpha^*\alpha_0\right], \\ p^{(-)}(m,\alpha) &= |\langle m|D^{\dagger}(\alpha)|-\alpha_0\rangle|^2 \\ &= (m!)^{-1}|\alpha_0+\alpha|^{2m}\exp\left[-|\alpha|^2-|\alpha_0|^2-\alpha\alpha_0^*-\alpha^*\alpha_0\right], \\ \varepsilon(m,\alpha) &= 2(m!)^{-1}(-1)^m\exp\left[-|\alpha|^2-|\alpha_0|^2\right] \\ &\quad \mathrm{Re}[(-|\alpha_0|^2+|\alpha|^2+\alpha\alpha_0^*-\alpha^*\alpha_0)^m\exp\left[\alpha^*\alpha_0-\alpha\alpha_0^*\right]]\,. \end{aligned} \tag{30}$$

In Fig. 2(b), we take the contour plot of the original Wigner function $W(\alpha, \alpha^*)$ and reconstruct it in Fig. 4. As we begin to increase the value of κ, the Wigner function becomes closer and closer to the original one. This behavior of the recovery of Wigner function is just like the same as the recovery of photon statistics. For the slit opening $\delta x = 1/4$, and $\kappa = 45$ the reconstructed graphs show good agreement with original Wigner function.

IV. OFF-RESONANT ATOM FIELD INTERACTION

In this section we discuss the situation where the standing wave field, inside the cavity, encodes information in the center of mass momenta of the off-resonant out going atoms in Raman-Nath regime. Again we suppose a quantized field in a cavity with a slit in front of it. A beam of two-level atoms having detuning $\Delta = \upsilon - \omega_{ab}$ interacts with the cavity field. The υ is the frequency of the field mode inside the cavity and ω_{ab} is the atomic transition frequency. For the Raman-Nath regime, the transverse motion of the atoms during interaction is ignored which allows us to drop the kinetic energy term in the Hamiltonian. The issue involved in this section is essentially used for analyzing quantum non-demolition measurement [18]. The atom-field interaction Hamiltonian in Schrödinger picture under dipole and rotating wave approximation is given by

$$H = \frac{\hbar\Delta}{2}\sigma_z + \hbar g \sin(k\hat{x}) \left(\sigma_+ a + a^\dagger \sigma_-\right), \tag{31}$$

where $\sigma_z = |a\rangle \langle a| - |b\rangle \langle b|$ is the inversion operator. In the limit of large detuning Δ, we derive the effective Hamiltonian for the atom-field interaction [19],

$$H_{eff} = \frac{\hbar\Delta}{2}\sigma_z + \frac{\hbar g^2 \sin^2(k\hat{x})}{\Delta} \left(\sigma_z a^\dagger a + \sigma_+ \ \sigma_-\right). \tag{32}$$

In deriving the above Hamiltonian, for large detuning limit we mean $g^2 m/\Delta^2 << 1$ [23]. For the sake of simplicity, we use the effective Hamiltonian in the following calculations. The equations of motion for the density matrix elements are

$$\dot{\rho}_{a,a}^{m-1,m-1}(x', x, t) = i\frac{g^2 m}{\Delta} \left(\sin^2(kx) - \sin^2(kx')\right) \rho_{a,a}^{m-1,m-1}(x', x, t), \tag{33}$$

$$\dot{\rho}_{b,b}^{m,m}(x',x,t) = -i\frac{g^2 m}{\Delta}\left(\sin^2(kx) - \sin^2(kx')\right)\rho_{b,b}^{m,m}(x',x,t). \tag{34}$$

In the above set of equations, the off-diagonal density matrix element (the terms $\rho_{a,b}^{m-1,m}(x',x,t)$ and $\rho_{b,a}^{m,m-1}(x',x,t)$) are absent due to the approximation of the large detuning limits. Furthermore, the equations of motion for density matrix elements of the excited and ground state atoms are independent of each other, thus we can formally integrate them to get the result. The supposition, that the atoms are in ground state and they are highly detuned with the cavity field lead us to conclude that they remain in ground state after the interaction with the cavity field. That is why we need to solve the equation (34) only. The formal solution of this equation is

$$\rho_{b,b}^{m,m}(x',x,t) = \exp\left[-i\frac{g^2 mt}{\Delta}\left(\sin^2(kx) - \sin^2(kx')\right)\right]\rho_{b,b}^{m,m}(x',x,0). \tag{35}$$

Following the same procedure as in the case of resonant atom-field interaction (section III), we take the Fourier transform of the equation (35) from position space to momentum space in normalized co-ordinates, the resultant equation is

$$\begin{aligned}\rho_{b,b}^{m,m}(\wp,t) = \frac{1}{2\pi\hbar}\int_{-\infty}^{\infty}\int_{-\infty}^{\infty}\frac{d\theta}{k}\frac{d\theta'}{k}\rho_{b,b}^{m,m}(\theta',\theta,0) \\ \times\exp\left[-i\frac{g^2 mt}{\Delta}\left(\sin^2(\theta) - \sin^2(\theta')\right) + i\wp\left(\theta-\theta'\right)\right].\end{aligned} \tag{36}$$

In order to have a linear term in trigonometric expression we use a well known relation $\sin^2(\theta) = (1+\cos(2\theta))/2$. While doing the proposed experiment we focus the atomic beam in the mid way between node and antinode of the standing wave cavity field, and during the calculation we replace θ with $\theta + \pi/4$. We further propose the small opening of the slit as compared to the wavelength of the standing wave cavity field. This approximation allows us to replace $\sin(kx)\tilde{=}kx$. All this results

$$\sin^2(\theta) = \frac{1}{2} + \theta, \tag{37}$$

and

$$\sin^2(\theta') = \frac{1}{2} + \theta'. \tag{38}$$

By putting these values in equation (36), we get

$$\rho_{b,b}^{m,m}(\wp,t)=\frac{1}{2\pi\hbar}\int_{-\infty}^{\infty}\int_{-\infty}^{\infty}\frac{d\theta}{k}\frac{d\theta'}{k}\rho_{b,b}^{m,m}(\theta',\theta,0)$$
$$\times\exp\left[-i\frac{g^2mt}{\Delta}\left(\theta-\theta'\right)+i\wp\left(\theta-\theta'\right)\right]. \tag{39}$$

At this stage we separate θ and θ' parts of the above equation. We choose the same initial condition as described in the resonant atom-field interaction in section III. We get the momentum distribution of the atomic probe by taking the trace over the field and atomic states. As in the large detuning limit, we have only the ground stated atoms at the detection screen, so the momentum distribution of them is given by

$$W'(\wp)=\sum_m\left(\left|\sqrt{\frac{1}{2\pi\hbar}}\int_{-\infty}^{\infty}\frac{d\theta}{k}g\left(\frac{\theta}{k}\right)\exp\left[-i\left(\frac{g^2tm}{\Delta}-\wp\right)\theta\right]\right|^2p(m)\right). \tag{40}$$

The integration of the above equation with $g\left(\frac{\theta}{k}\right)$ (which is expressed in equation (24)) is carried out. The result found is

$$W'(\wp)=\sum_m\left|\left(\frac{\delta x^2}{\pi\hbar^2}\right)^{\frac{1}{4}}\exp\left[-\delta x^2k^2\left(\kappa'm-\wp\right)^2\right]\right|^2p(m), \tag{41}$$

where $\kappa'=g^2t/\Delta$. It is clear from the above equation that the momentum distribution has a peak when m becomes equal to $\wp/\kappa'$. While in the resonant atom-field interaction peaks come at the points where $\sqrt{m}$ is equal to $\wp/\kappa$. The plots of the momentum distribution and the recovered photon statistics for the case when Schrodinger-cat state is present in the cavity are given in Fig. 5. In the present case, the peaks of the momentum distribution become resolved at very small value of κ' as compared to the resonant case. The Fig. 5(a) shows the momentum distribution and 5($a^{'}$) the recovered photon statistics for $\kappa'=5$. Here the peaks of the momentum distribution are not fully resolved which causes the partial recovery of the photon statistics. The situation is better for $\kappa'=7$ in Fig. 5(b), showing that for stronger field coupling of atom-field interaction, one can have the resolved peak spectrum of momentum distribution at detection screen. The situation is more favorable if we consider relatively higher value for $\kappa'=10$ as shown in Fig. 5(c), where the photon statistics is fully recovered. In all these graphs, the slit width is chosen as $\delta x=1/4$.

For the recovery of the Wigner function, we displace the photon statistics of the cavity field by injecting the coherent state from local classical oscillator. The displaced photon statistics $p'_r(m,\alpha)$ is recovered from the momentum distribution via

$$p'_r(m,\alpha) = \left\{ \frac{1}{\mathcal{M}'} W'(\wp)|_{\wp=\kappa' m} \quad \text{for } m \geq 0, \right. \tag{42}$$

where $\mathcal{M}'$ is a normalization constant, and is then used to reconstruct the Wigner distribution function of the cavity field. The expression of the displaced photon statistics $p'_r(m,\alpha)$ is given by equation (30) for Schrödinger-cat state. We reconstruct the Wigner function of Schrödinger-cat state for $\kappa' = 5, 7$ and 10, with $\delta x = 1/4$. The graphs show that as we increase the value of κ' from 5 to 10, the contour plots of Wigner function approaches to the original one. We get the exact replica of the original function for $\kappa' = 10$ which is shown in Fig. 6(c).

V. RESULTS AND DISCUSSIONS

We have recovered the photon statistics of the cavity field in the case of Schrödinger-cat state for both the resonant and off-resonant atom-field interaction. The graphs are taken for initial Gaussian distribution of the atoms at the slit. The original photon statistics of the cavity field is plotted in Fig. 2(a) for $\xi = 3$, and the Wigner function for $\alpha = 2$ is shown in Fig. 2(b). First, while considering the resonant atom-field interaction, we note that when κ is increased from 25 to 45 gradually, the peaks in the momentum distribution spectrum begin to resolve. The opening of the slit has the reverse behavior on the momentum distribution spectrum, i.e., as we decrease the width of the slit, the more strength of the coupling is needed. We have used the limit that the slit has smaller width as compared to the wavelength of the cavity field. This allows us to replace the $\sin(kx)$ dependence by linear kx dependence. We use $\delta x = 1/4$ of the wavelength of the cavity field which is a valid approximation under the existing limit. We find the photon statistics of the cavity field with the help of the resolved spectrum of the momentum distribution. The Fig. 3(a) shows

the momentum distribution of the atoms and $3(a')$ is the recovered photon statistics of the cavity field for $\kappa = 25$. Here the peaks of the momentum distribution are not fully resolved which causes the partial recovery of the photon statistics of the cavity field. Although the positions of the peaks in recovered photon statistics match with the original but the heights remain different. The reconstruction becomes relatively better at $\kappa = 35$ (i.e., $3(b')$) and is fully recovered for the case when $\kappa = 45$ in $3(c')$ where the peaks of the momentum distribution are fully resolved.

For the case of off-resonant atom-field interaction, we need smaller values of κ' as compared to the resonant case to resolve the peaks in momentum distribution. We present the relevant graphs of the recovery for the photon statistics of the Schrödinger-cat state in Fig. 5. The values used for the slit opening and the photon statistics of the cavity field are same as they were used in the case of resonant atom-field interaction, but here we need just $\kappa' = 10$ for the best reconstruction of the photon statistics.

In order to recover the Wigner function, we displace the photon statistics of the cavity field by injecting coherent state by a local classical oscillator. The Wigner function of the cavity field for resonant atom field interaction has recovered completely for $\kappa = 45$. However, for lower values of κ, the partial recovery of the Wigner function is observed. The comparative graphs of the recovered Wigner function for different values of κ is shown in Fig. 4. We also reconstruct the Wigner function of the cavity field for the off-resonant atom-field interaction. In the off-resonant case for $\kappa' = 10$ (in Fig. $6(c)$), we get the full recovery of the Wigner function and for $\kappa' = 5$ and 7 the partial recovery which is plotted in Fig. 6(a) & (b), respectively.

In conclusion we have proposed a scheme for the reconstruction of the photon statistics and hence for the Wigner function of the quantized cavity field for both the resonant and off-resonant atom-field interaction. We observe that in case of off-resonant atom field interaction a small value of κ is sufficient to observe the resolved peak spectrum in momentum distribution of out going atoms. While on the other hand, we need relatively large value of κ for the case of resonant atom-field interaction. The advantage of the presented scheme is

that it works well for the case of mixed state also. The parameters chosen for the reconstruction of the photon statics and the Wigner function are attainable in current state of art.

Acknowledgment

Authors would like to acknowledge the financial support of Pakistan Science Foundation.

REFERENCES

[1] P. A. M. Dirac, *The Principles of Quantum Mechanics* (Clarendon Press, Oxford, 1958).

[2] See the reprint W. Pauli, *General Principles of Quantum Mechanics* (Springer, Berlin, 1980).

[3] Matthias Freyberger and Stefan H. Kienle Phys. Rev. A **56** 195 (1997).

[4] For a review on squeezed states, see K. Zaheer and M. S. Zubairy, in *Advances in Atomic, Molecular, and Optical Physics*, Vol. 28, ed. by D. Bates and B. Bederson, (Academic Press, New York 1991), p. 143.

[5] E. Schrödinger, Naturwissenschaften **23** 807 (1935); **23** 823 (1935); **23** 844 (1935) [English translation by J. D. Trimmer, Proc. Am. Phys. Soc. **124**, 3325 (1980)].

[6] K. Vogel and H. Risken, Phys Rev. A **40**, 2847 (1989).

[7] G. M. D'Ariano, U. Leonhardt, and H. Poul, Phys. Rev. A **52**, R1801 (1995). U. Leonhardt, H. Paul, and G. M. D'Ariano, ibid. **52**, 4899 (1995); Mashhood Ahmad, Shahad Qamar and M. S. Zubairy, Phys. Rev. A **62**, 43814 (2000).

[8] M. Brune, S. Haroche, V. Lefevre, J. M. Raimond, and N. Zagury, Phys. Rev. Lett. **65**, 976 (1990).

[9] M. J. Holland, D. F. Walls, and P. Zoller, Phys. Rev. Lett. **67**, 1716 (1991).

[10] A. M. Herkommer, V. M. Akulin and W. P. Schleivh, Phys. Rev. Lett. **69**, 3298 (1992).

[11] M. Freyberger and A. M. Herkommer, Phys. Rev. Lett.**72**, 1952 (1994).

[12] P. J. Bardroff, E. Mayr, and W. P. Schleich, Phys. Rev. A **51**, 4963 (1995); W.Vogel, D.-G. Welsch, and L. Leine, J. Opt. Soc. Am. B **4**, 1633 (1987).

[13] M. S. Zubairy, Phys. Lett. A **222**, 91 (1996).

[14] M. S. Zubairy, Phys. Rev. A **57**, 2066 (1998); T. Azim and M. S. Zubairy, Phys. Lett.

A **250**, 344 (1998).

[15] L. G. Lutterbach and L. Davidovich, Phys. Rev. Lett. **78**, 2547 (1997); C. T. Bodendorf, G. Antesberger, M. S. Kim, and H. Walther, Phys. Rev. A **57**, 1371 (1998); M. S. Kim, C. T. Bodendorf, G. Antesberger, and H. Walther, Phys. Rev. A **58**, R65 (1998).

[16] See, for example, M. O. Scully and M. S. Zubairy, in *Quantum Optics*, (Cambridge University Press, 1997).

[17] K. E. Cahill and R. J. Glauber, Phys. Rev. A **177**, 1857 (1969); *ibid* A **177**, 1882 (1969).

[18] N. Imoto, H. A. Haus, and Y. Yamamoto, Phys. Rev. A **32**, 2287 (1985).

[19] S. M. Tan and D. F. Walls, Phys. Rev. A **47**, 663 (1993).

[20] S. Schnider, A. M. Herkommer, U. Leonhardt and W. P. Schleich, J. Mod. Opt. **44,** 2333 (1997).

[21] D. T. Smithey, M. Beck, M. G. Raymer and A. Faridani, Phys. Rev. Lett. **70**, 1244 (1993).

[22] S. Schiller, G. Breitenbach, S. F. Pereira, T. Muller and J. Mlynek, Phys. Rev. Lett. **77**, 2933 (1996).

[23] M. Brune, S. Haroche, J. M. Raimond, L. Davidovich and N. Zagury, Phys. Rev. A **45,** 5193 (1992).

Figure caption

Fig. 1: Schematics of the proposed two-level atoms interacting with the quantized cavity field. A slit of width δx is placed to collimate the atomic beam on the small region of the standing wave cavity field. The atoms pass through the slit in their ground state $|b\rangle$. After the atom-field interaction the atomic momenta is detected by the velocity selectors.

Fig. 2: (a) The photon statistics of the Schrödinger-cat state which we would like to measure for $\xi = 3$. (b) The Wigner function $W(\alpha, \alpha^*)$ of the cavity field where we choose $\alpha = 2$.

Fig. 3: Momentum distribution $W(\wp)$ versus the scaled momentum $\wp/\kappa$. (a) the momentum distribution of the atoms after atom-field interaction, for $\kappa = 25$. $(a^{'})$ the partial recovery of the original photon statistics, here the peaks of the photon statistics occur at their proper place but the height do not match with the original one (see Fig 2. (a)). The momentum distribution is relatively resolved in (b), with better recovery of the photon statistics in $(b^{'})$ for the case when $\kappa = 35$. For $\kappa = 45$, the momentum distribution become sharply peaked (c) and the plot of the recovered photon statistics of the cavity field $(c^{'})$ becomes in good agreement with original one. In all these cases the slit width $\delta x = 1/4$ is used.

Fig. 4: The reconstructed Wigner distribution function $W_r(\alpha, \alpha^*)$ of Schrödinger-cat state. (a) the reconstructed contour plot of the Wigner function of the Schrödinger-cat state for $\kappa = 25$. Here the Wigner function of the cavity field is disturbed. (b) is for $\kappa = 35$, and recovery is still not matching with the original. (c) shows the situation when we choose $\kappa = 45$ where the original Wigner function is fully recovered. For all the graphs, the slit opening $\delta x = 1/4$ of the wavelength of the cavity field is employed.

Fig. 5: The momentum distribution of the atoms and the reconstructed photon statistics of the cavity field in case of large detuning limit. We take the graphs of the momentum distribution for $\kappa' = 5$, 7, and 10, with $\delta x = 1/4$ in (a), (b) and (c), respectively. The recovered photon statistics in $(a^{'})$, $(b^{'})$ and $(c^{'})$ correspond to momentum distribution (a),

(c) and (f). As we increase the value of κ' the momentum distribution goes on to be sharply peaked. These sharp peaks in the momentum distribution are exploited for the recovery of photon statistics.

Fig. 6: The reconstructed Wigner function in case of large detuning limit, with $\alpha_0 = 2$, and the slit width $\delta x = 1/4$. (a) is recovered Wigner function for $\kappa' = 5$, (b) is for $\kappa' = 7$, in these figures the Wigner function do not agree with the original, where the (c) is plotted for $\kappa' = 10$ and shows the full recovery of the original Wigner function.

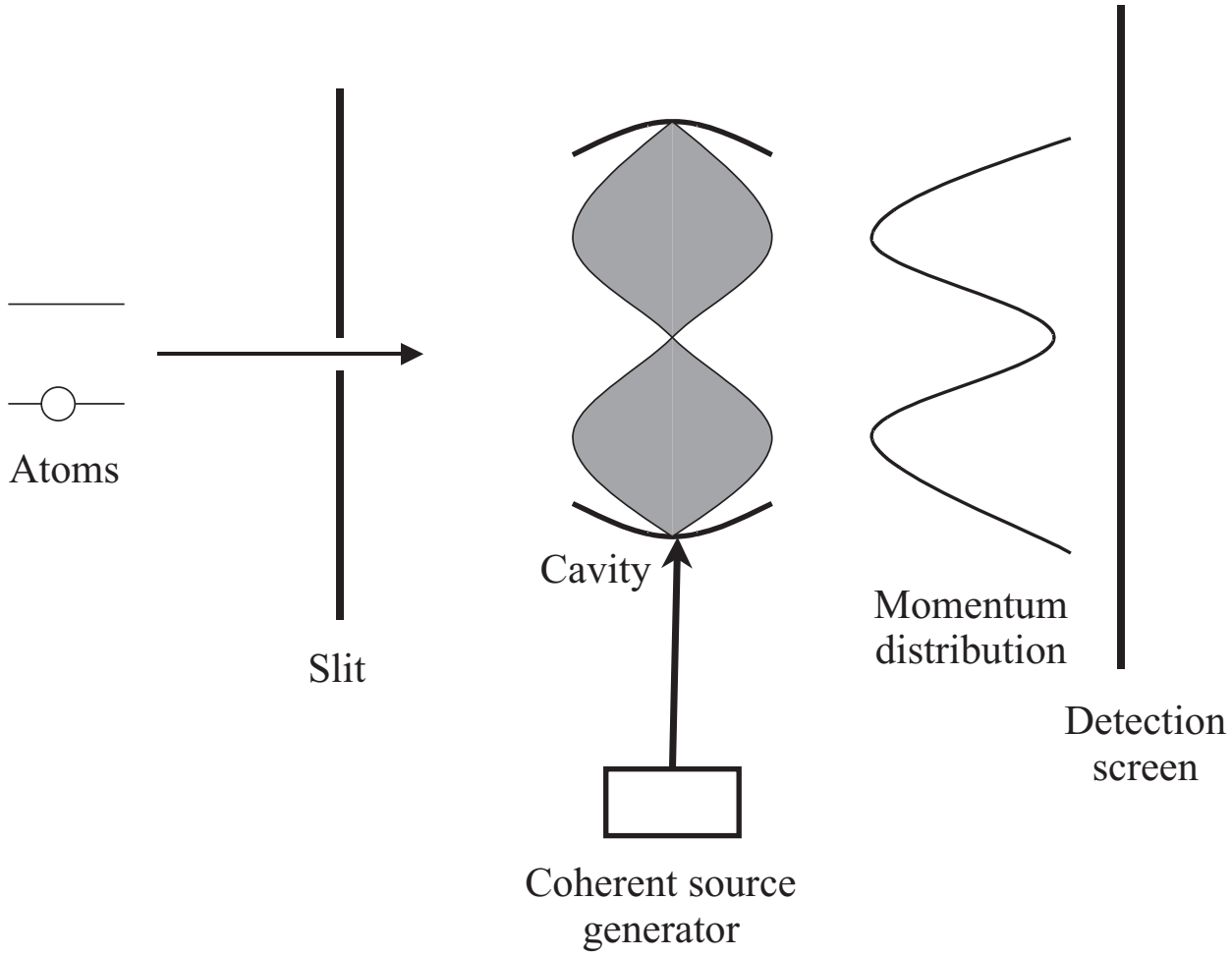
Atoms
Slit
Cavity
Momentum
distribution
Detection
screen
Coherent source
generator

Fig. 1

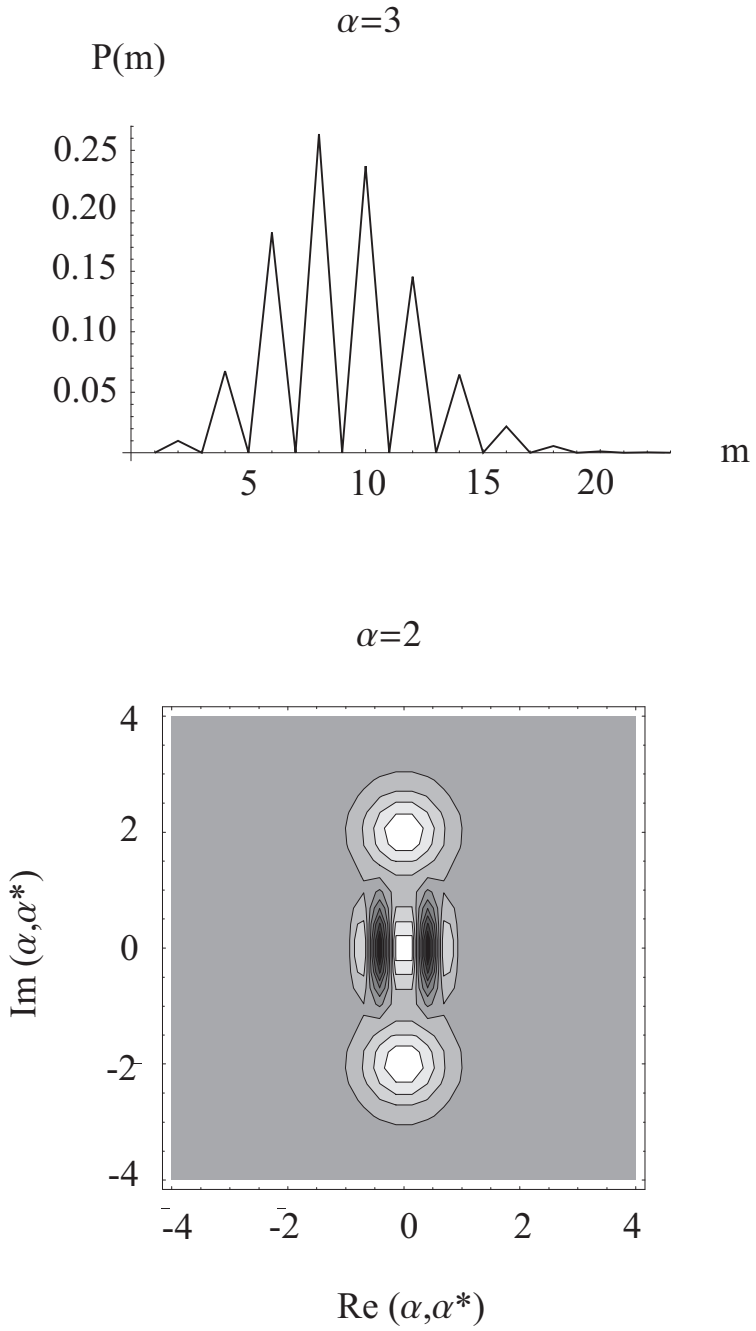

Fig. 2.

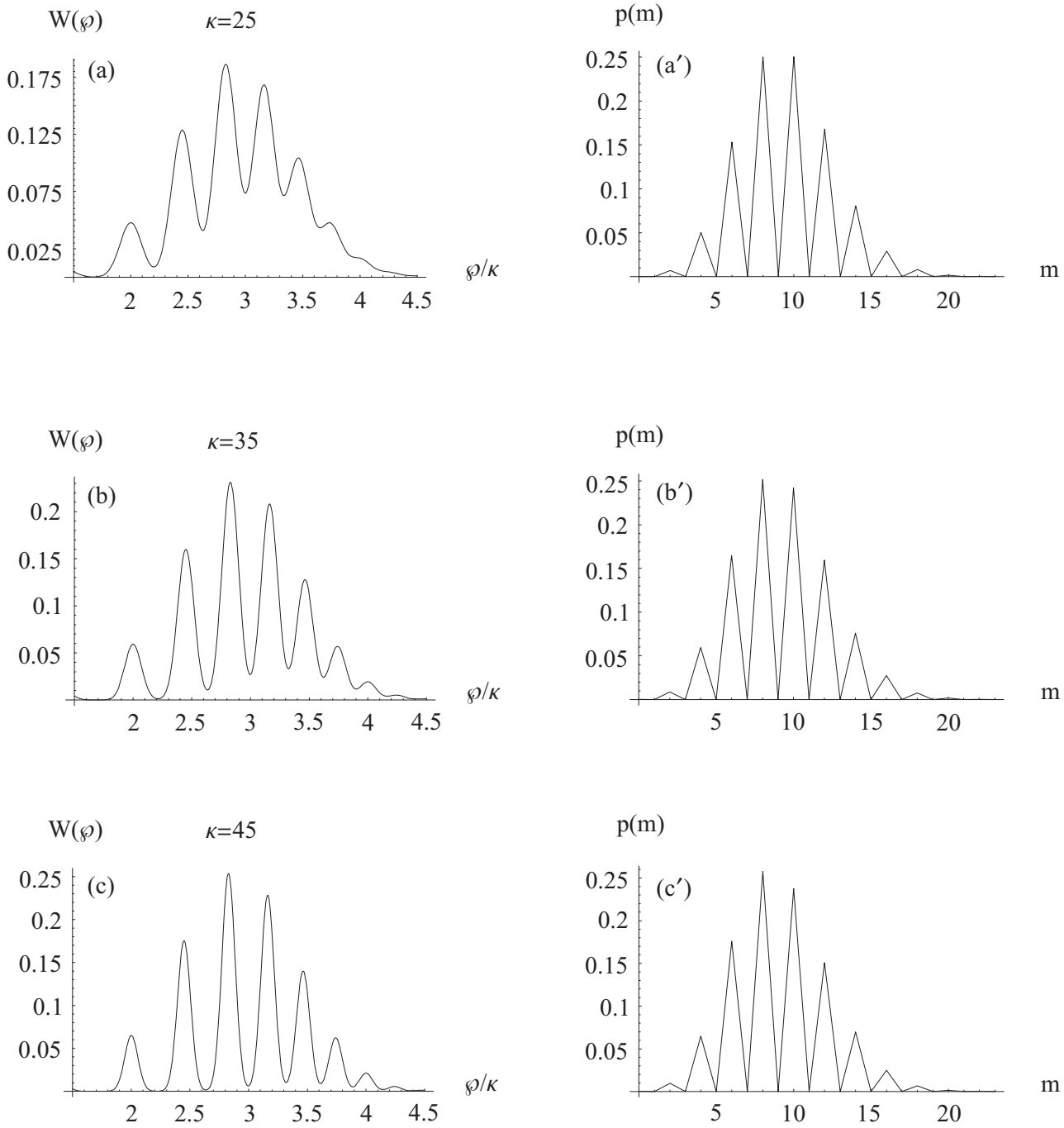
W(φ)
κ=25
(a)
0.175
0.125
0.075
0.025
2
2.5
3
3.5
4
4.5
φ/κ
p(m)
(a′)
0.25
0.2
0.15
0.1
0.05
5
10
15
20
m
W(φ)
κ=35
(b)
0.2
0.15
0.1
0.05
2
2.5
3
3.5
4
4.5
φ/κ
p(m)
(b′)
0.25
0.2
0.15
0.1
0.05
5
10
15
20
m
W(φ)
κ=45
(c)
0.25
0.2
0.15
0.1
0.05
2
2.5
3
3.5
4
4.5
φ/κ
p(m)
(c′)
0.25
0.2
0.15
0.1
0.05
5
10
15
20
m

Fig. 3.

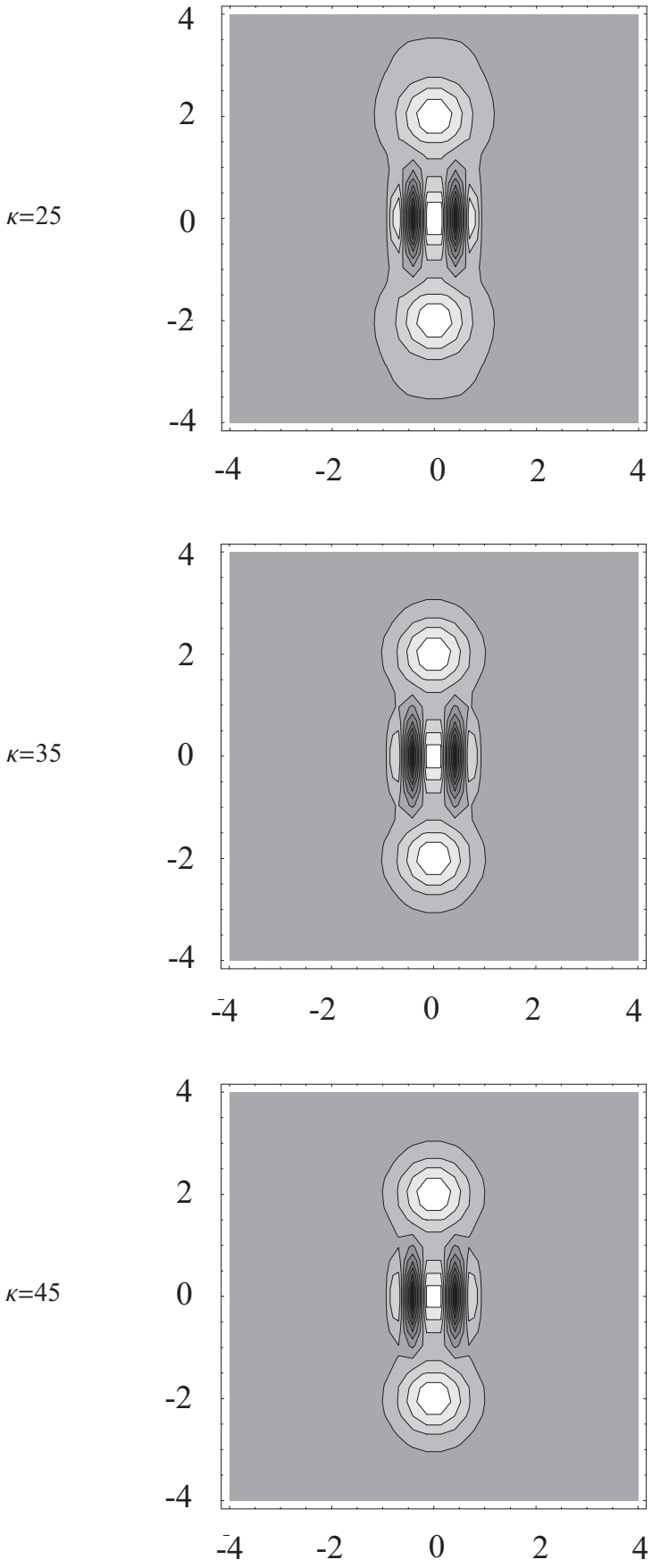

Fig. 4.

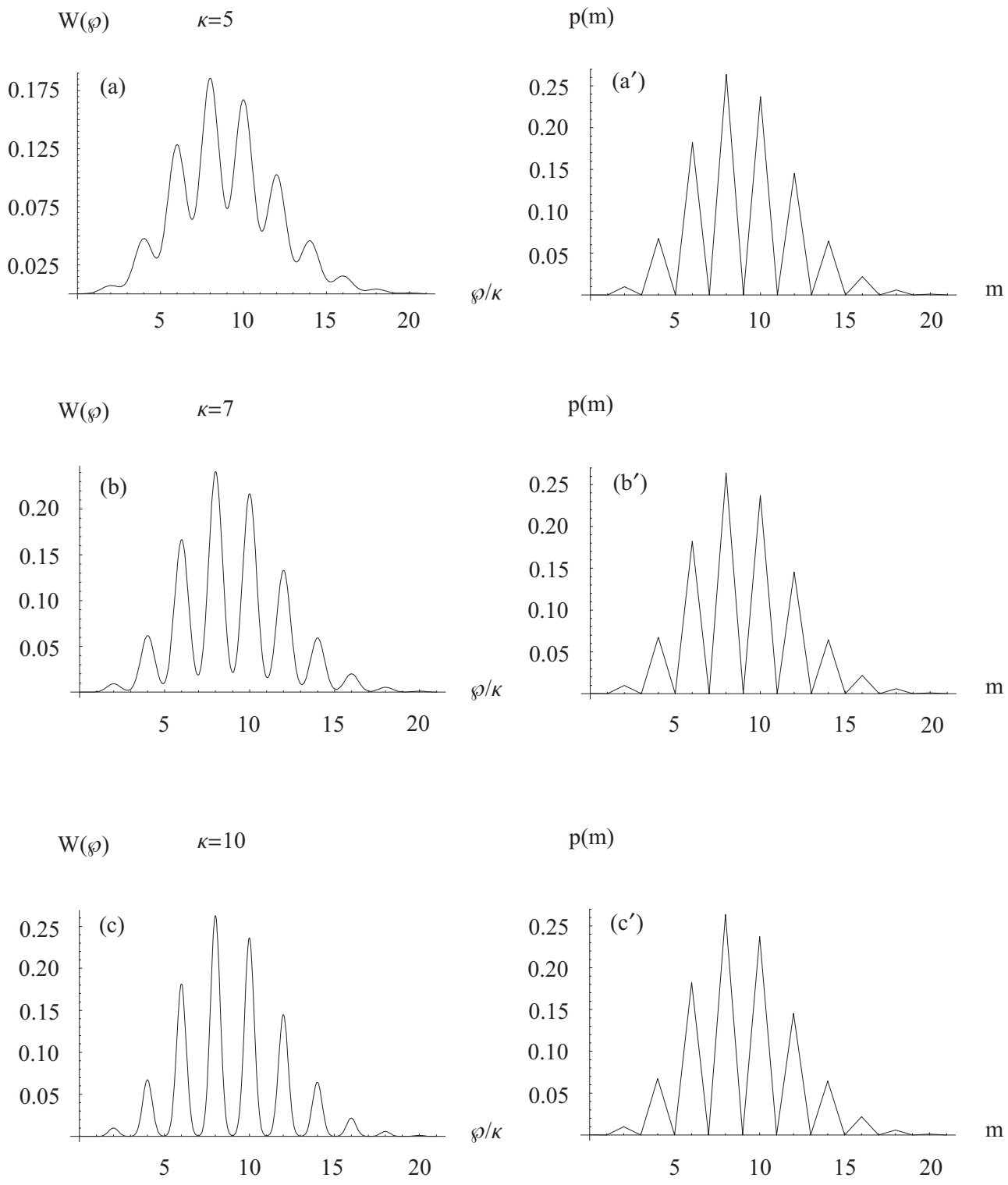
W(φ)
κ=5
(a)
0.175
0.125
0.075
0.025
5
10
15
20
φ/κ
p(m)
(a′)
0.25
0.20
0.15
0.10
0.05
5
10
15
20
m
W(φ)
κ=7
(b)
0.20
0.15
0.10
0.05
5
10
15
20
φ/κ
p(m)
(b′)
0.25
0.20
0.15
0.10
0.05
5
10
15
20
m
W(φ)
κ=10
(c)
0.25
0.20
0.15
0.10
0.05
5
10
15
20
φ/κ
p(m)
(c′)
0.25
0.20
0.15
0.10
0.05
5
10
15
20
m

Fig. 5.

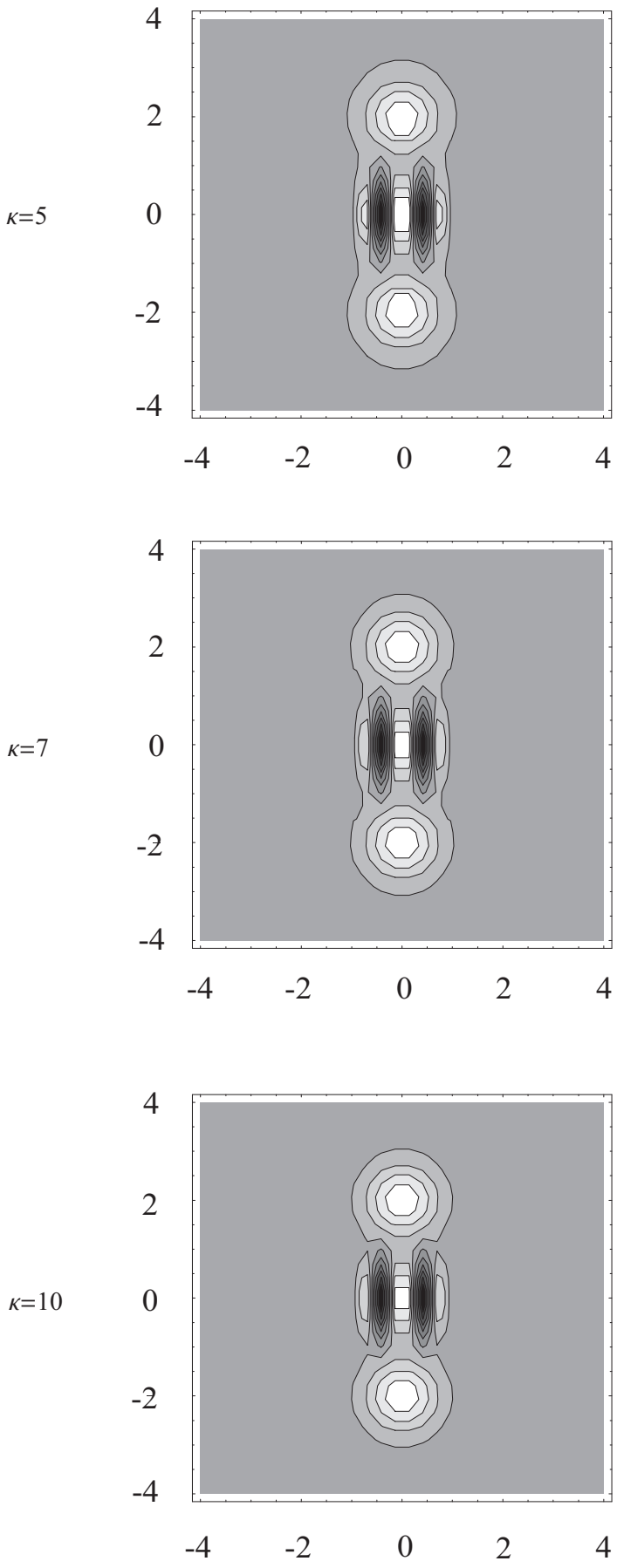

Fig. 4.